Orbital-Ordering-Induced Ferroelectricity in $SrCrO_3$

Kapil Gupta,[1] Priya Mahadevan,[1,*] Phivos Mavropoulos,[2] and Marjana Ležaić[2]

[1]*S. N. Bose National Centre for Basic Sciences, Block JD, Sector-III, Saltlake, Kolkata 700 098, India*

[2]*Peter Grünberg Institut and Institute for Advanced Simulation, Forschungszentrum Jülich and JARA, D-52425 Jülich, Germany*

(Received 1 February 2012; revised manuscript received 7 May 2013; published 15 August 2013)

Using density functional theory calculations, ultrathin films of $SrVO_3(d^1)$ and $SrCrO_3(d^2)$ on $SrTiO_3$ substrates have been studied as possible multiferroics. Although both are metallic in the bulk limit, they are found to be insulating as a result of orbital ordering driven by lattice distortions at the ultrathin limit. While the distortions in $SrVO_3$ have a first-order Jahn-Teller origin, those in $SrCrO_3$ are ferroelectric in nature. This route to ferroelectricity results in polarizations comparable with conventional ferroelectrics.

DOI: 10.1103/PhysRevLett.111.077601 PACS numbers: 77.80.−e, 71.15.Mb, 75.85.+t

Recent advances in the growth of oxide thin films have allowed one to engineer both electronic and magnetic functionalities in oxides, very different from their bulk counterparts [1–5]. This additional dimension of oxide research has opened up the possibility of generating cross-correlated electronic couplings which could be interchangeably controlled by both electric as well as magnetic fields, generating new classes of multiferroics. In contrast, there are very few examples among bulk materials which are both magnetic as well as ferroelectric. This is because ferroelectricity (FE) is usually found in d^0 systems and d^0-ness is not compatible with magnetic order [6]. There are examples of systems which exhibit both orders among finite d^n systems; however, the magnitudes of polarization are usually small in such cases.

An avenue that has been quite successful as a route to new ferroelectrics in thin films is one where substrate strain and overlayer thickness have been used as handles to modify properties, resulting in behavior very different from the bulk. The work by Haeni *et al.* [7] showed that substrate strain could be used to engineer a ferroelectric ground state in $SrTiO_3$, a d^0 paraelectric. While it was not obvious that this route should also work for multiferroics, first-principles calculations [8] predict that the strain induced by merely depositing the room-temperature ferrimagnetic double perovskites Bi_2NiReO_6 and Bi_2MnReO_6 on a substrate should turn their antipolar bulk ground state into a ferroelectric one. S. Bhattacharjee *et al.* [9] showed theoretically that by increasing the lattice constant of $CaMnO_3$, a polar mode becomes soft and almost degenerate with an antipolar mode. Similar observations were made in epitaxially strained simple binary oxides such as BaO and EuO [10] as well as $BaMnO_3$ [11], $SrMnO_3$ [12], and $EuTiO_3$ [13,14], none of which are examples of bulk ferroelectric materials. All these examples were band insulators. Therefore, Jahn-Teller effects were irrelevant in these systems, allowing, under strain, for the manifestation of the pseudo-Jahn-Teller effects, which are usually associated with noncentrosymmetric distortions. An important consequence of these studies was that ferroelectric polarization as large as that found in d^0 ferroelectrics was predicted in these oxides. In contrast, the observed ferroelectric polarization in most multiferroics is at least 1 or more orders of magnitude lower [15–17]. This route to a high polarization and possibly magnetism associated with the same atom opens up interesting possibilities.

Orbital ordering has recently emerged as an alternate route to FE. This was recently realized in films of doped manganites on a high-index surface of the substrate [18], where orbital ordering with an axis tilted away from the substrate normal was found. This led to off centering. Again, in this case, the examples considered were bulk insulators, which we show in the present work need not be a limitation in the choice of materials. We start by considering the example of $SrVO_3$ and $SrCrO_3$, both of which are metallic in the bulk. In this work, we explore a new route to non-d^0 FE through ultrathin films of transition-metal oxides which, as discussed earlier, were found to be insulating. In contrast to the examples listed above, in the cases we investigate, the transition-metal cation is Jahn-Teller active in bulk. A further important difference is that strain (although it could be present) does not play a crucial role in the induced FE.

Ultrathin films [just two monolayers (MLs)] of $SrVO_3$ on $SrTiO_3$ (001) as well as films comprising two MLs of $SrCrO_3$ on $SrTiO_3$ (001) are considered. Examining the electronic structure theoretically, we find both systems to be insulating, both arising from an orbital ordering at the surface, driven primarily by structural distortions. While $SrVO_3$ favors Jahn-Teller distortions, $SrCrO_3$ favors a ferroelectric ground state, with a large contribution to the energy lowering in the insulating state derived from these distortions. Our detailed analysis shows that the modifications of the crystal field at the surface associated with a missing apical oxygen allow for the observed FE in $SrCrO_3$ (and possibly in other non-d^0 transition-metal compounds). These distortions at the surface survive even for the thicker films. The calculated polarization is found to be large, comparable to that in bulk d^0 ferroelectrics.

We consider a symmetric slab (see, for instance, Ref. [19]) consisting of 13 layers of SrO-TiO_2, terminating

in a TiO_2 layer, to mimic the substrate. The in-plane lattice constant is fixed at the experimental value (3.905 Å) for $SrTiO_3$, while the out-of-plane lattice constant was varied. We allowed for tilts of the TiO_6 as well as MO_6 octahedra, a distortion observed in low-temperature $SrTiO_3$ [20]. The electronic structure of these systems was calculated within VASP [21] using a k-point mesh of $6 \times 6 \times 1$ using a generalized gradient approximation (GGA) + U scheme [22,23] with a U_{eff} of 2.2/2.5 on V/Cr [24]. A vacuum of 15 Å was used to minimize interaction between slabs in the periodic supercell geometry. Internal positions were allowed to relax to their minimum energy value. We construct maximally localized Wannier functions and use the shifts of their centers in the ferroelectric phase with respect to the paraelectric one to calculate the ferroelectric polarization [25]. For this purpose, the electronic ground state for the relaxed structure was converged with the full-potential linearized augmented plane wave method-based code FLEUR [26], in film geometry, on a 7×7 k-point mesh. The maximally localized Wannier functions were constructed with the WANNIER90 code [27] and the interface between FLEUR and WANNIER90 [28]. The advantage of the Wannier functions approach (over the Berry phase one) in the specific system where the ferroelectric polarization is not uniform is that the contributions of every layer or atom (see Ref. [28]) to the electronic polarization can be extracted.

We started by calculating the electronic structure of bulk $SrVO_3$ and $SrCrO_3$ within GGA + U. Both compounds were found to be metallic, consistent with experiment. Next, we performed similar calculations for two MLs of $SrMO_3$ (M = V, Cr) on $SrTiO_3$, and the ground state was in both cases found to be insulating.

Let us first examine in more detail the case of $SrVO_3$. Each VO_5 unit at the surface has in-plane V-O bond lengths (1.95 Å) longer than the out-of-plane one (1.91 Å). This could in principle result in a lower energy for the d_{xy} orbital than for the doubly degenerate d_{yz} and d_{xz} orbitals [Fig. 1(a)]. As there is just one electron associated with the V^{4+} ion, in this case, an insulating ground state is expected. However, since one of the apical oxygens is missing at the surface, this could result in a reversed ordering of the levels leading to a metallic state [Fig. 1(b)]. Our calculations find the scenario discussed in Fig. 1(b) realized. However, on performing a complete structural optimization, one finds an orbital-ordering transition which has a Jahn-Teller origin with two elongated V-O (2.18 Å) and two contracted V-O bond lengths (1.78 Å) [see Fig. 1(c)]. A ferromagnetic state is found to be favored by 60 meV/V at the two-ML limit, in contrast to the bulk, which is paramagnetic.

To contrast the results for $SrVO_3$ films, we have also considered two MLs of $SrCrO_3$ on a $SrTiO_3$ substrate. Here, the degeneracy lifting of the Cr t_{2g} levels is also a consequence of the missing apical oxygen with the d_{xz} and

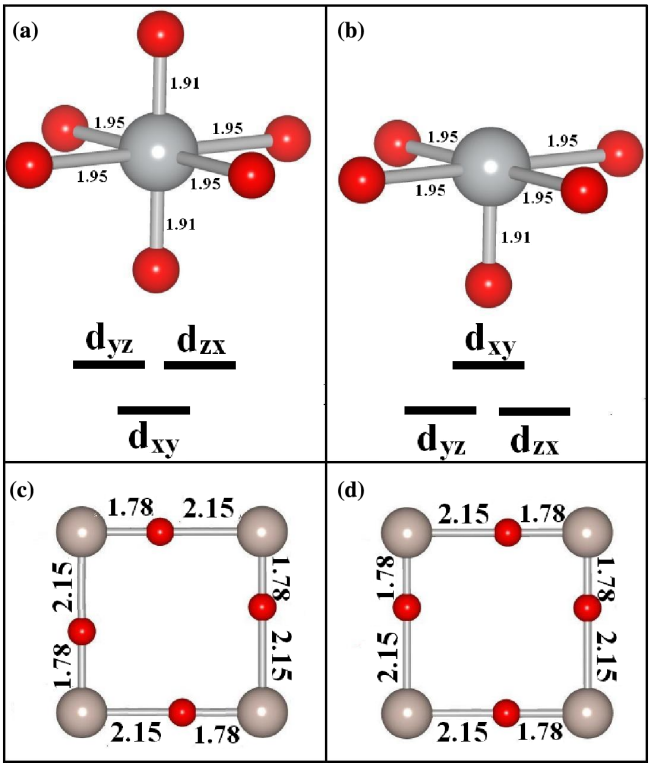

FIG. 1 (color online). Distortions and crystal field splitting of the t_{2g} orbitals for (a) a MO_6 octahedron under tensile strain and (b) a surface MO_5 unit, where M = transition-metal atom. The M-O network in the x-y plane found in the presence of (c) Jahn-Teller distortions (seen in $SrVO_3$) and (d) pseudo-Jahn-Teller distortions (seen in $SrCrO_3$). Large (small) and gray (red) spheres denote M (O) atoms.

d_{yz} levels at lower energy than the d_{xy} level. As there are two electrons in the d levels of the Cr^{4+} ion, they occupy the doubly degenerate d_{xz} and d_{yz} levels, leading to a band insulator. Interestingly, we find that carrying out complete structural optimization results in a strong modification of the in-plane Cr-O bond lengths from their starting values: while two of the bond lengths contract, the other two extend [Fig. 1(d)] [29]. The effect of this structural distortion is that the system has no inversion symmetry now and possesses a finite electric polarization. While in both $SrVO_3$ and $SrCrO_3$ the dominant energy lowering comes from the in-plane distortions, note the important difference: in $SrCrO_3$, the Jahn-Teller effect is quenched due to one additional electron on the Cr^{4+} cation and to the modified crystal field at the surface (with respect to that of the bulk material), so the pseudo-Jahn-Teller effects become operative, driving the system ferroelectric or polar. These results put ultrathin films of $SrCrO_3$ in the same category of band insulators turned ferroelectrics where orbital ordering drives the system insulating. Now, every band insulator does not turn ferroelectric, so this immediately brings up the question of the microscopic interactions that are responsible for FE here. In the following,

we investigate the origin of the observed ferroelectric distortions.

In Fig. 2(a), we have plotted the partial density of Cr-d states for the structure in which the film is constrained to be centrosymmetric. A band gap barely opens up in this structure between the majority spin Cr d_{yz}/d_{xz} states and the d_{xy} states. The bandwidths associated with the d_{xz} and d_{yz} orbitals are a factor of 2 less than the bandwidths associated with the d_{xy} orbitals as a result of broken periodicity along the positive z direction. Allowing for the constraint of centrosymmetry to be relaxed, we find that two of the in-plane Cr-O bond lengths become shorter and are equal to 1.78 Å while two others become longer and are equal to 2.15 Å, in contrast to their undistorted values of 1.95 Å. A part of the energy lowering in the process comes from the increased hopping interaction due to shorter Cr-O bonds. This is clearly seen in the increased separation of the bonding and antibonding states with dominant contribution from the d_{xy} orbitals [Fig. 2(b)]. The shorter Cr-O bond lengths also result in an increased repulsion between the electrons on Cr and O. This is partly overcome by the presence of the vacuum in the z direction, which allows the d_{xz} and d_{yz} orbitals to extend into the vacuum region. This may be seen from the charge density plot associated with the antibonding states with d_{xz}/d_{yz} character plotted in the inset of Fig. 2(b). The lobe of the d orbital closer to the longer Cr-O bond extends further into the vacuum to compensate for the increased repulsion associated with the shorter Cr-O bonds. These results also provide us with design principles for generating multiferroic materials in which one has MO_5 structures resulting from MO_6 octahedra. In-plane distortions as well as larger spacings in one of the z directions in which the oxygen is absent could result in ferroic distortions.

In Fig. 3, we show the calculated values of the layer-resolved ferroelectric polarization for the case of two MLs of $SrCrO_3$ on $SrTiO_3$. The bars with the vertical (violet) pattern show the total (ionic plus electronic) polarization in CrO_2/TiO_2 layers, while the ones with the horizontal (green) pattern show the total polarization in SrO layers. The (gray) bars outlined with violet (CrO_2/TiO_2 layers) or green (SrO layers) indicate the electronic contribution to the total polarization in the respective layers. Note that the electronic contribution in CrO_2/TiO_2 layers is rather large. It constitutes about 50% of the total polarization, while in SrO layers it is smaller and negative. The polarization points in the $\langle 110 \rangle$ direction (in plane) and is calculated per layer; i.e., instead of the unit cell volume that would be used to evaluate it in a bulk system, we use the volume of each layer, calculated as the product of the area of the in-plane unit cell and the sum of the half-distances to the neighboring layers on either side. The volume of the surface layer is taken to be equal to the one beneath it. While not ferroelectric in bulk, we find that a significant polarization is induced in high-k $SrTiO_3$ by the ferroelectric shifts of Cr^{4+} ions at the surface. Note that the polarization in the center of the film is constrained to zero by the chosen geometry (in the calculation, the Cr^{4+} ions move in the opposite directions on the opposite sides of the film), and its decay with the distance from the surface need not be as rapid in the case of a thicker substrate. A rough estimate of the energy for switching is found to be 42 meV [30], similar to other displacive ferroelectrics [31].

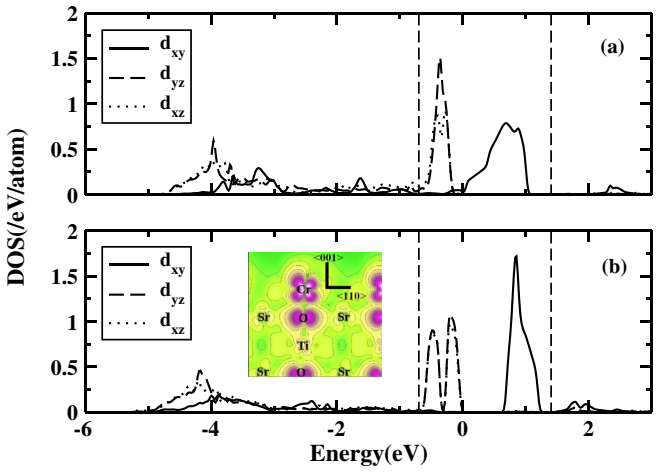

FIG. 2 (color online). The majority spin d_{xz}, d_{yz}, and d_{xy} projected partial density of states for a Cr atom (a) in bulklike geometry and (b) in the optimized ferroelectric geometry for two MLs of $SrCrO_3$ films on $SrTiO_3$. The charge density associated with the antibonding states with d_{xz} and d_{yz} character is shown in inset of (b). Vertical dashed lines indicate the valence band maximum and conduction band minimum of $SrTiO_3$. The zero of energy indicates the Fermi energy.

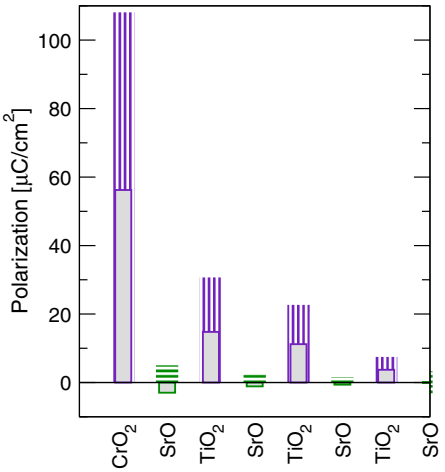

FIG. 3 (color online). The layer resolved polarizations for two MLs of $SrCrO_3$ on $SrTiO_3$: The bars with a vertical violet pattern show the total (ionic plus electronic) polarization in CrO_2 layers, while the ones with the horizontal green pattern show the total polarization in SrO layers. The gray bars outlined with violet (CrO_2 layers) or green (SrO layers) indicate the electronic contribution to the total polarization in the respective layers.

In $SrCrO_3$, the observed ferroelectric distortions were associated with the two-ML limit. However, when an additional SrO ML was added, this led to the out-of-plane distortions becoming the largest distortions. The differing environments on either side of the surface CrO_6 octahedra lead to unequal bond lengths of 1.88 and 1.95 Å along the positive and negative z directions. As a result, a finite dipole moment develops (although it is unswitchable by an electric field). Similar observations have been made on other interfaces [32]. The system still remains insulating at this limit. Adding another layer, we find that the surface CrO_2 layer sustains ferroelectric distortions in addition to charge ordering. The Cr in CrO_2 is found to have a negative charge transfer energy [33]. Here, we also find this to be the case, and consequently, some of the holes are localized on the oxygens. The surface Cr atoms are found to have a valency of $d^{1+\delta}$ and d^2 [Figs. 4(a) and 4(b)], while the subsurface Cr atoms have a breathing-mode-type distortion which leads to a valency of $d^{3-\delta}$ and d^2 on these Cr atoms [Figs. 4(c) and 4(d)]. By comparing the total energy of several configurations, we find a ferromagnetic coupling parameter in the surface Cr layer and an antiferromagnetic coupling in the subsurface layer and between the layers.

In the preceding discussion, the substrate imposed a tensile strain on the $SrCrO_3$ overlayers. It is impressive, however, that one finds that as a consequence of the large stabilization energy for the in-plane ferroelectric distortions, the films can sustain these distortions even for 2% compressive strain.

Having established FE at the ultrathin limit, we went on to examine the magnetic properties as a function of thickness. The bulk is found to be an antiferromagnetic metal,

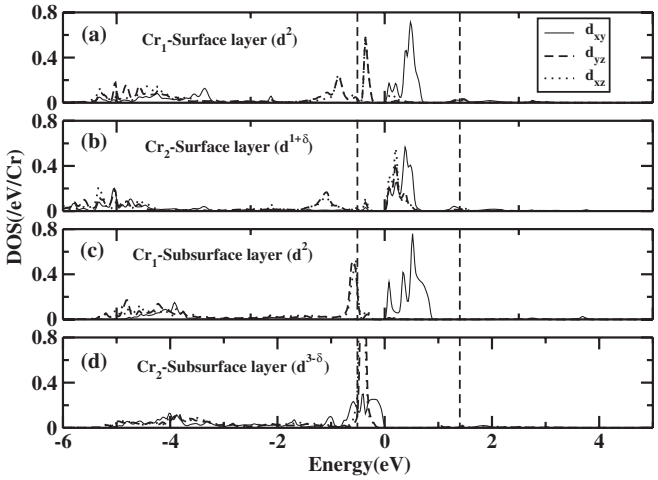

FIG. 4. The majority spin d_{xz}, d_{yz}, and d_{xy} projected partial density of states for a Cr atom belonging to (a),(b) the surface layer and to (c),(d) the subsurface layer of four-ML $SrCrO_3$ films on $SrTiO_3$. Vertical dashed lines indicate the valence band maximum and conduction band minimum of $SrTiO_3$. The zero of energy indicates the Fermi energy.

consistent with experiment. At the ultrathin limit of two MLs, the antiferromagnetic state is more stable than the ferromagnetic state by 45 meV/Cr atom, corresponding to a nearest-neighbor coupling of $J = 11.25$ meV in a Heisenberg model. The stabilization of an antiferromagnetic state can be easily understood within a superexchange picture, as there are channels for delocalization only for an antiferromagnetic arrangement of spins. This difference is enhanced at the three-ML limit to 52 meV/Cr atom. At the four-ML limit, various magnetic configurations were considered, and we find that the surface layer becomes ferromagnetic while the subsurface CrO_2 layer becomes antiferromagnetic, with the system found to be insulating. The closely competing configuration where both surface layer Cr atoms as well as the subsurface layer Cr atoms are coupled antiferromagnetically is found to be 9 meV/Cr atom higher.

From a device perspective, the important question is whether there is a coupling between the electrical and magnetic degrees of freedom. We compute the magnetic crystalline anisotropy for the two-ML film of $SrCrO_3$ and find that the spin favors an in-plane orientation over an out-of-plane one by 128 μeV per Cr atom. Within the plane, the spin favors an orientation at 90° to the direction of the electric polarization by 14 μeV. We note that a similar arrangement was observed in $BiFeO_3$ [34]. By Monte Carlo simulations on a Heisenberg model basis, including single-ion anisotropy, we find that the coupling between electric polarization and staggered-magnetization direction persists up to a temperature of 70 K, after which short-range magnetic order is lost. Even if this temperature is considerably lower than room temperature, the novel mechanism that is revealed here could emerge in other materials at higher temperature, provided that the exchange is stronger.

Ultrathin films of d^1 and d^2 transition-metal oxides have been explored as possible candidates for multiferroicity. Orbital ordering allows one to realize an insulating surface even in systems where the bulk form is metallic. While these have a Jahn-Teller origin in the case of $SrVO_3$, pseudo-Jahn-Teller effects result in sizeable ferroelectric distortions for $SrCrO_3$ which, even in the absence of strain, also turns out to be an antiferromagnetic insulator at this limit of two MLs. These distortions persist into the substrate and survive for the surface CrO_5 layer even for thicker films of four MLs opening up new possibilities for non-d^0 multiferroics.

We acknowledge useful discussions with D. D. Sarma, S. Blügel, and I. B. Bersuker. K. G. acknowledges CSIR, India, and P. M. acknowledges DST, Government of India, through the Indo-EU Project ATHENA for financial support. M. L. gratefully acknowledges the financial support of the Young Investigators Group Programme of the Helmholtz Association, Contract No. VH-NG-409, the support of the Jülich Supercomputing Centre and the

European Community's Seventh Framework Programme (FP7/2007-2013) under Grant No. NMP3-LA-2010-246102. P. M. and M. L. also thank the DST-DAAD programme which funded the exchange visits.

*Corresponding author.
priya@bose.res.in

[1] A. Ohtomo and H. Hwang, Nature (London) **427**, 423 (2004); J. T. Heron, M. Trassin, K. Ashraf, M. Gajek, Q. He, S. Y. Yang, D. E. Nikonov, Y.-H. Chu, S. Salahuddin, and R. Ramesh, Phys. Rev. Lett. **107**, 217202 (2011).
[2] P. Allen, H. Berger, O. Chauvet, L. Forro, T. Jarlborg, A. Junod, B. Revaz, and G. Santi, Phys. Rev. B **53**, 4393 (1996); G. Cao, S. McCall, M. Shepard, J. E. Crow, and R. P. Guertin, Phys. Rev. B **56**, 321 (1997).
[3] P. Mahadevan, F. Aryasetiawan, A. Janotti, and T. Sasaki, Phys. Rev. B **80**, 035106 (2009).
[4] K. Yoshimatsu, T. Okabe, H. Kumigashira, S. Okamoto, S. Aizaki, A. Fujimori, and M. Oshima, Phys. Rev. Lett. **104**, 147601 (2010).
[5] R. Scherwitzl, S. Gariglio, M. Gabay, P. Zubko, M. Gibert, and J.-M. Triscone, Appl. Phys. Lett. **95**, 222114 (2009); Phys. Rev. Lett. **106**, 246403 (2011).
[6] N. A. Hill, J. Phys. Chem. B **104**, 6694 (2000).
[7] J. H. Haeni *et al.*, Nature (London) **430**, 758 (2004).
[8] M. Ležaić and N. A. Spaldin, Phys. Rev. B **83**, 024410 (2011).
[9] S. Bhattacharjee, E. Bousquet, and P. Ghosez, Phys. Rev. Lett. **102**, 117602 (2009).
[10] E. Bousquet, N. A. Spaldin, and P. Ghosez, Phys. Rev. Lett. **104**, 037601 (2010).
[11] J. M. Rondinelli, A. S. Eidelson, and N. A. Spaldin, Phys. Rev. B **79**, 205119 (2009).
[12] J. H. Lee and K. M. Rabe, Phys. Rev. Lett. **104**, 207204 (2010).
[13] C. J. Fennie and K. M. Rabe, Phys. Rev. Lett. **97**, 267602 (2006).
[14] J. H. Lee *et al.*, Nat. Mater. **466**, 954 (2010).
[15] T. Kimura, T. Goto, H. Shintani, K. Ishizaka, T. Arima, and Y. Tokura, Nature (London) **426**, 55 (2003).
[16] L. C. Chapon, G. R. Blake, M. J. Gutmann, S. Park, N. Hur, P. G. Radaelli, and S.-W. Cheong, Phys. Rev. Lett. **93**, 177402 (2004).
[17] G. Lawes *et al.*, Phys. Rev. Lett. **95**, 087205 (2005).
[18] N. Ogawa, Y. Ogimoto, Y. Ida, Y. Nomura, R. Arita, and K. Miyano, Phys. Rev. Lett. **108**, 157603 (2012).
[19] R. I. Eglitis and D. Vanderbilt, Phys. Rev. B **77**, 195408 (2008).
[20] F. W. Lytle, J. Appl. Phys. **35**, 2212 (1964).
[21] G. Kresse and J. Furthmüller, Phys. Rev. B **54**, 11 169 (1996); G. Kresse and J. Furthmüller, Comput. Mater. Sci. **6**, 15 (1996).
[22] J. P. Perdew, in *Electronic Structure of Solids*, edited by P. Ziesche and H. Eschrig (Akademie Verlag, Berlin, 1991), p. 11.
[23] S. L. Dudarev, G. A. Botton, S. Y. Savrasov, C. J. Humphreys, and A. P. Sutton, Phys. Rev. B **57**, 1505 (1998).
[24] F. Aryasetiawan, M. Imada, A. Georges, G. Kotliar, S. Biermann, and A. I. Lichtenstein, Phys. Rev. B **70**, 195104 (2004).
[25] R. D. King-Smith and David Vanderbilt, Phys. Rev. B **47**, 1651 (1993).
[26] http://www.flapw.de.
[27] A. A. Mostofi, J. R. Yates, Y.-S. Lee, I. Souza, D. Vanderbilt, and N. Marzari, Comput. Phys. Commun. **178**, 685 (2008).
[28] F. Freimuth, Y. Mokrousov, D. Wortmann, S. Heinze, and S. Blugel, Phys. Rev. B **78**, 035120 (2008).
[29] See Supplemental Material at http://link.aps.org/supplemental/10.1103/PhysRevLett.111.077601 for other starting configurations, which were found to have a higher energy or to be difficult to converge.
[30] The ferroelectric simulation cell has an energy of 0.84 eV above the centrosymmetric one. As all transition-metal atoms show off centering, dividing by the number of transition-metal atoms gives us a rough idea of the energy for flipping.
[31] R. E. Cohen, Nature (London) **358**, 136 (1992).
[32] G. Singh-Bhalla, C. Bell, J. Ravichandran, W. Siemons, Y. Hikita, S. Salahuddin, A. F. Hebard, H. Y. Hwang, and R. Ramesh, Nat. Phys. **7**, 80 (2011).
[33] M. A. Korotin, V. I. Anisimov, D. I. Khomiskii, and G. A. Sawatzky, Phys. Rev. Lett. **80**, 4305 (1998).
[34] S. H. Baek *et al.*, Nat. Mater. **9**, 309 (2010).